5-2004

Dissociation Potential Curves of Low-Lying States in Transition Metal Hydrides. 2. Hydrides of Groups 3 and 5

Shiro Koseki
Osaka Prefecture UniVersity

Yohei Ishihara
Osaka Prefecture UniVersity

Dmitri G. Fedorov
National Institute of Advanced Industrial Science and Technology

Hiroaki S. Umeda
National Institute of Advanced Industrial Science and Technology

Michael Schmidt
Iowa State University, mike@si.fi.ameslab.gov

Dissociation Potential Curves of Low-Lying States in Transition Metal Hydrides. 2. Hydrides of Groups 3 and 5

Abstract
The dissociation energy curves of low-lying spin-mixed states for Group 5 hydrides (VH, NbH, and TaH), as well as Group 3 hydrides (ScH, YH, and LaH), have been calculated by using both effective core potential (ECP) and all-electron (AE) approaches. The two approaches are based on the multiconfiguration self-consistent field (MCSCF) method, followed by second-order configuration interaction (SOCI) calculations: the first method employs an ECP basis set proposed by Stevens and co-workers (SBKJC) augmented by a set of polarization functions, and spin−orbit coupling effects are estimated with a one-electron approximation, using effective nuclear charges. The second method employs a double-ζ basis set developed by Huzinaga (MIDI) and three sets of p functions are added to both transition element and hydrogen and one set of f functions is also added to the transition element. The relativistic elimination of small components (RESC) scheme and full Breit−Pauli Hamiltonian are employed in the AE approaches to incorporate relativistic effects. The present paper reports a comprehensive set of theoretical results including the dissociation energies, equilibrium distances, electronic transition energies, harmonic frequencies, anharmonicities, and rotational constants for several low-lying spin-mixed states in the hydrides, filling a considerable gap in available data for these molecules. Transition moments are also computed among the spin-mixed states, and qualitative agreement is obtained for Group 3 hydrides in comparison with the experimental results reported by Ram and Bernath. Peak positions of emission spectra in Group 5 hydrides are also predicted.

Disciplines
Chemistry

Comments
Reprinted (adapted) with permission from *Journal of Physical Chemistry A* 108 (2004): 4707, doi:10.1021/jp049839h.

Authors
Shiro Koseki, Yohei Ishihara, Dmitri G. Fedorov, Hiroaki S. Umeda, Michael Schmidt, and Mark S. Gordon

Dissociation Potential Curves of Low-Lying States in Transition Metal Hydrides. 2. Hydrides of Groups 3 and 5

Shiro Koseki,*,† Yohei Ishihara,† Dmitri G. Fedorov,‡ Hiroaki Umeda,‡,§ Michael W. Schmidt,⊥ and Mark S. Gordon*,⊥

Department of Material Science, Osaka Prefecture University, 1-1 Gakuen-cho, Sakai, Osaka 599-8531, Japan, National Institute of Advanced Industrial Science and Technology and Grid Technology Research Center, 1-1-1 Umezono, Tsukuba, Ibaraki 305-6568, Japan, and Department of Chemistry, Iowa State University, Ames, Iowa 50011

Received: January 13, 2004; In Final Form: March 13, 2004

The dissociation energy curves of low-lying spin-mixed states for Group 5 hydrides (VH, NbH, and TaH), as well as Group 3 hydrides (ScH, YH, and LaH), have been calculated by using both effective core potential (ECP) and all-electron (AE) approaches. The two approaches are based on the multiconfiguration self-consistent field (MCSCF) method, followed by second-order configuration interaction (SOCI) calculations: the first method employs an ECP basis set proposed by Stevens and co-workers (SBKJC) augmented by a set of polarization functions, and spin−orbit coupling effects are estimated with a one-electron approximation, using effective nuclear charges. The second method employs a double-ζ basis set developed by Huzinaga (MIDI) and three sets of p functions are added to both transition element and hydrogen and one set of f functions is also added to the transition element. The relativistic elimination of small components (RESC) scheme and full Breit−Pauli Hamiltonian are employed in the AE approaches to incorporate relativistic effects. The present paper reports a comprehensive set of theoretical results including the dissociation energies, equilibrium distances, electronic transition energies, harmonic frequencies, anharmonicities, and rotational constants for several low-lying spin-mixed states in the hydrides, filling a considerable gap in available data for these molecules. Transition moments are also computed among the spin-mixed states, and qualitative agreement is obtained for Group 3 hydrides in comparison with the experimental results reported by Ram and Bernath. Peak positions of emission spectra in Group 5 hydrides are also predicted.

1. Introduction

High levels of theoretical calculations have become possible due to the rapid development of new algorithms and computational power. The estimation of relativistic effects is one of the targets in such high-level theoretical calculations, and various practical approximations have been proposed recently that are suitable for molecular calculations.[1] Several recent excellent reviews discuss these approximations[2−7] in detail. In addition, useful quantum chemistry program codes are available to the public, so that it becomes easy to estimate relativistic effects in molecules of moderate size.

Recent theoretical investigations have frequently been performed on the electronic structure of chemical compounds including heavy metal elements and on their chemical reactivity. It is important to understand the role of d electrons in chemical bond formation and cleavage,[8−21] and relativistic effects often play dominant roles in such processes. To enable an entry level of theory, we have proposed effective nuclear charges for the first- through sixth-row main-group elements, as well as those for the first- through third-row transition elements, to estimate spin−orbit splittings within the one-electron (Z_{eff}) approximation.[22−28] Although higher levels of relativistic theories are nowadays available for the estimation of spin−orbit coupling effects, it is time-consuming to apply such high levels of theory to large molecular systems. Therefore, the Z_{eff} approximation is still useful for estimating spin−orbit coupling effects in large molecular systems. Of course, it is sensible to investigate the reliability of the Z_{eff} approximation in comparison with results obtained at higher levels of theory, as well as with experimental observations. The previous study (Part I of this series) reported on Group 4 hydrides, TiH, ZrH, and HfH,[28] in which multiconfiguration self-consistent field (MCSCF) methods were employed and followed by second-order configuration interaction (SOCI) calculations, using limited external spaces. We concluded that the one-electron approximation[22,26,27] performed very well for TiH and ZrH, but the agreement between the effective core potential (ECP) and all-electron (AE) results is somewhat worse for HfH.

The present paper is the second in the series; the reliability of the ECP and AE methods is examined by using applications to Group 5 hydrides (VH, NbH, and TaH), together with Group 3 hydrides (ScH, YH, and LaH). All calculations have been performed with the GAMESS suite of program codes.[29,30]

2. Methods of Calculation

Both effective core potential (ECP) and all-electron (AE) calculations were carried out with multiconfiguration self-consistent field (MCSCF) wave functions[31,32] followed by second-order configuration interaction (SOCI) calculations.[33]

* To whom correspondence should be addressed. E-mail: shiro@ms.cias.osakafu-u.ac.jp; mark@si.fi.ameslab.gov.
† Osaka Prefecture University.
‡ National Institute of Advanced Industrial Science and Technology.
§ Grid Technology Research Center.
⊥ Iowa State University.

10.1021/jp049839h CCC: $27.50
Published on Web 05/01/2004

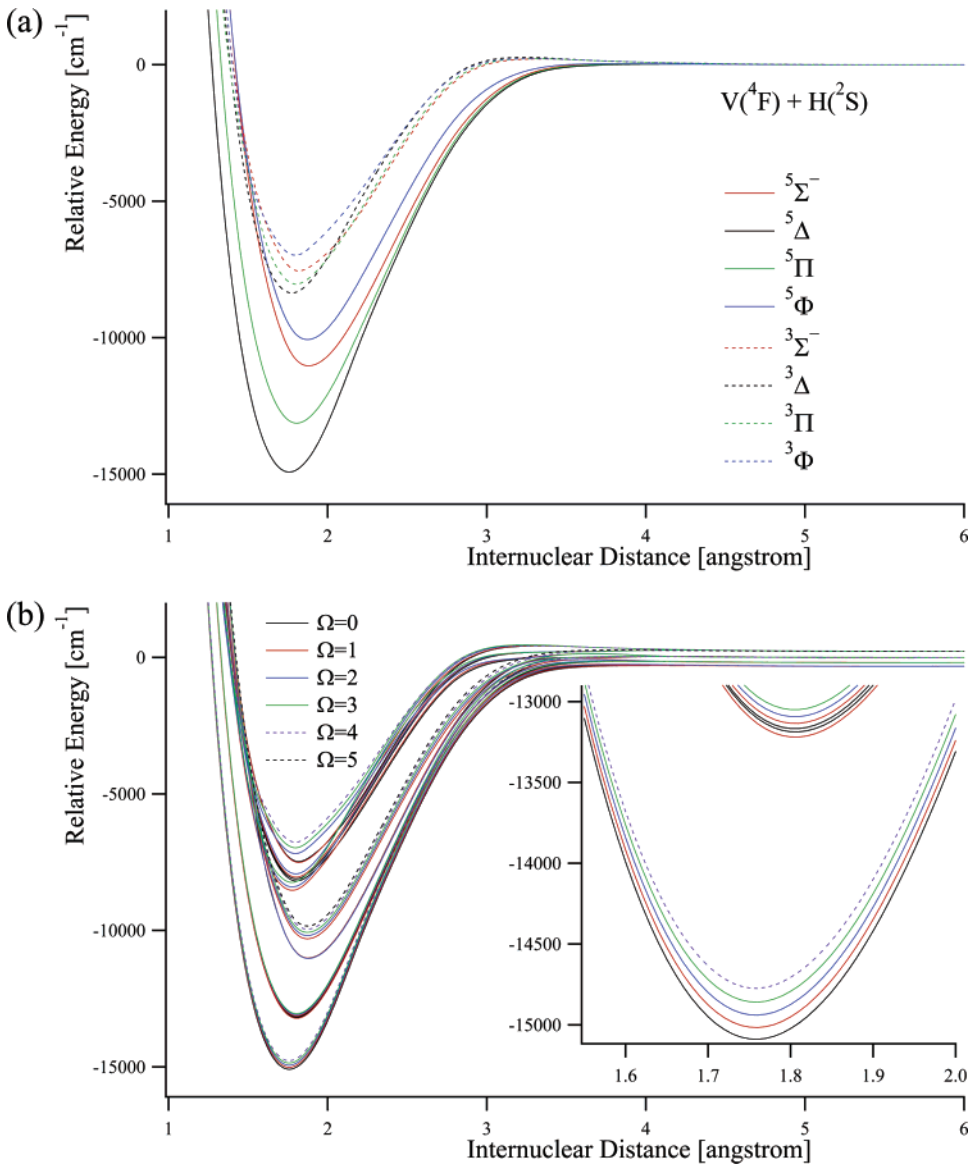

Figure 1. VH potential energy curves obtained with use of quartet MCSCF+SOCI/SBKJC(f,p) wave functions: (a) low-lying adiabatic statesand (b) low-lying spin-mixed states. The inset figure is a close-up view near the energy minima.

The MCSCF active space included the orbitals corresponding to the *n*d and $(n + 1)$sp orbitals of the transition element and the 1s orbital of hydrogen, where "*n*" is the principal quantum number ($n = 3$, 4, and 5), for nearly all compounds. An exception is NbH ($n = 4$), for which it was found that only a 4d5d5s6s(Nb)+1s(H) active space correctly predicts atomic spectra. The orbitals were optimized by using the state-averaged MCSCF method with equal weights for the lowest four states ($^5\Sigma^-$, $^5\Pi$, $^5\Delta$, and $^5\Phi$) of VH, the lowest three states ($^5\Sigma^+$, $^5\Pi$, and $^5\Delta$) of NbH, or three states ($^1\Sigma^+$, $^1\Pi$, and $^1\Delta$) for Group 3 hydrides. These states correlate with the ground state of the transition element in the dissociation limit.[34] Since it was found that the ground state of TaH is a triplet based on the orbital optimization for either triplets or quintets, all results presented below were obtained with the MCSCF orbitals optimized for the lowest four triplet states ($^3\Sigma^-$, $^3\Pi$, $^3\Delta$, and $^3\Phi$) with equal weights.

The MCSCF optimized orbitals were employed in SOCI calculations to construct singlet, triplet, quintet, and septet wave functions and to estimate spin−orbit couplings among these wave functions. Although *all external orbitals were used in the SOCI calculations of Group 3 hydrides*, the external space in the SOCI calculations of Group 5 hydrides included only the 13 orbitals that correlate with the $(n + 1)$d, $(n + 2)$s, and $(n + 2)$p orbitals for the transition element and with 2s and 2p orbitals for hydrogen in the dissociation limit, where these external orbitals are the lowest eigenvectors of the standard MCSCF Fock operator. This is necessitated by resource limitations. The spin−orbit coupling matrices include low-lying SOCI states. To construct spin−orbit coupling matrices of reasonable size, an energy tolerance was set for the excitation energy. All states within the energy range restricted by the tolerance were included, so that the number of states varied slightly for each method.[35] The estimated errors caused by the energy tolerance are about 3 (VH), 40 (NbH), and 450 (TaH) cm^{-1}, and less than 1 (ScH), 5 (YH), and 24 (LaH) cm^{-1} in Group 3 hydrides, respectively, on the basis of second-order perturbation theory using the largest matrix elements. For each molecule, the ground state within the LS coupling scheme and the lowest spin-mixed states are given in the tables discussed below, in which Ω is the *z* component of the total angular momentum quantum number.

The ECP calculations employed the SBKJC basis set,[36−39] augmented by a set of f functions[40] for the transition element.

TABLE 1: Spectroscopic Parameters for the Low-Lying Adiabatic and Spin-Mixed States in VH[a]

state	method	D_e	R_e	T_e	ω_e	$\omega_e x_e$	B_e	α_e	μ_e	refs
$^5\Delta$	ECP	14923	1.758	0	1629	30.75	5.578	0.236	1.7064	
	AE	15709	1.762	0	1576	23.51	5.471	0.227	1.8124	
$^5\Pi$	ECP	13131	1.805	1792	1555	35.50	5.246	0.231		
	AE	15035	1.797	753	1551	24.64	5.257	0.221		
$^5\Sigma^-$	ECP	11033	1.878	3890	1466	35.27	4.781	0.211		
	AE	14095	1.827	1694	1511	25.61	5.083	0.219		
$^5\Phi$	ECP	10071	1.872	4852	1480	42.05	4.842	0.227		
	AE	13160	1.814	2629	1500	28.39	5.159	0.234		
spin-mixed states										
$\Omega = 0^+$	ECP	14766	1.758	0	1629	31.20	5.576	0.237		
	AE	15671	1.762	0	1575	25.05	5.473	0.232		
$\Omega = 0^-$	ECP	14766	1.758	0	1629	31.11	5.576	0.237		
	AE	15671	1.762	1	1574	24.14	5.470	0.229		
$\Omega = 1$	ECP	14693	1.758	72	1628	31.41	5.576	0.237		
	AE	15618	1.762	53	1573	25.06	5.471	0.233		
$\Omega = 2$	ECP	14617	1.758	149	1628	31.46	5.576	0.238		
	AE	15561	1.762	111	1572	24.85	5.469	0.232		
$\Omega = 3$	ECP	14670	1.758	230	1629	31.31	5.577	0.237		
	AE	15601	1.762	175	1573	24.62	5.470	0.231		
$\Omega = 4$	ECP	14771	1.758	315	1629	30.78	5.578	0.236		
	AE	15674	1.761	246	1576	23.55	5.471	0.227		
$^5\Delta$	B3LYP	22314	1.677		1658					49
	AE	14277	1.74		1609	43	5.6	0.21		50
	AE/MCSCF+CISD	18552	1.74		1590					51
	MCPF	18782	1.719		1635					52, 77
	RECP	18794	1.719		1635					53
	expt	17173								49
	expt	13291 ± 1087								54
	expt	14211 ± 1421								55
	expt	17181 ± 565								75

[a] D_e = dissociation energy [cm^{-1}], R_e = equilibrium distance [Å], T_e = electronic transition energy (energy difference of potential minima) [cm^{-1}], ω_e = harmonic frequency [cm^{-1}], $\omega_e x_e$ = anharmonicity [cm^{-1}], B_e and α_e = rotational constants [cm^{-1}], μ_e = electric dipole moment [debye]. See the text.

The 31G basis set augmented by a set of p functions was employed for hydrogen.[41] With use of SOCI wave functions, the spin−orbit splittings of low-lying states were estimated within the one-electron (Z_{eff}) approximation.[42] This method is referred to simply as ECP in the following discussion.

The AE calculations employed the MIDI basis set[43] augmented by three sets of $(n + 1)$p functions in both the transition element and hydrogen[44] and also by one set of f functions on the transition element. The RESC scheme[45,46] was used throughout all AE calculations, since a previous study[28] showed that scalar relativistic corrections are necessary in AE calculations. The internal uncontraction option in RESC was used only for TaH, as preliminary tests indicated it is not important in other cases. Spin−orbit coupling matrices were constructed by using the SOCI wave functions and Breit−Pauli Hamiltonian including both one- and two-electron terms. Relativistic corrections to the Breit−Pauli Hamiltonian were taken into account for both one- and two-electron operators except for TaH, where only the one-electron operator was modified since it is very time-consuming to introduce the internal uncontraction effects of the two-electron SOC integrals. The method is referred to simply as AE in the following discussion.

The dissociation energies (D_e) and equilibrium distances (R_e) were obtained by fitting to a parabolic function near the minima of each state. The electronic transition energies (T_e) were calculated as energy differences between potential minima. The harmonic frequencies (ω_e), anharmonicities ($\omega_e x_e$), and rotational constants (B_e and α_e) for the lowest vibrational states of electronic states were obtained on the basis of the numerical analyses of dissociation energy curves.[47] The energy of a rovibrational state for vibrational and rotational quantum numbers of "v" and "J" in each electronic state is given as

$$E(v,J) = E_e + G(v) + F_v(J) = E_e + \omega_e(v + {}^1/_2) - \omega_e x_e(v + {}^1/_2)^2 + \{B_e - \alpha_e(v + {}^1/_2)\}J(J + 1)$$

where E_e is an electronic energy and vibrational and rotational energies are approximated by $G(v) = \omega_e(v + {}^1/_2) - \omega_e x_e(v + {}^1/_2)^2$ and $F_v(J) = \{B_e - \alpha_e(v + {}^1/_2)\}J(J + 1)$ in the present study, respectively.

3. Results and Discussion

3.1. Potential Energy Curves for VH. Both ECP and AE methods predict that the VH ground state is $^5\Delta$ within the adiabatic scheme. The ECP potential energy curves of the lowest $^5\Sigma^-$, $^5\Delta$, $^5\Pi$, and $^5\Phi$ states are plotted in Figure 1a, where, in the dissociation limit, these states all correlate with the ground state [$V(^4F) + H(^2S)$]; the ground state of V has the electronic configuration $(3d)^3(4s)^2$. The AE curves are quite similar to the ECP ones, although the low-lying triplet states, correlating with the ground state in the dissociation limit, are closer in energy to the quintet states than are the ECP curves (see Figure 1S (Supporting Information)). Table 1 lists spectroscopic parameters in the quintet states obtained with both ECP and AE methods within the adiabatic scheme.

The adiabatic $^5\Delta$ ground state is split into six spin-mixed states ($\Omega = 0^+$, 0^-, 1, 2, 3, and 4) by spin−orbit coupling effects. As shown in Table 1, since the coupling is rather weak, the energy separation is small among the spin-mixed states and, as a result, the internuclear distances R_e do not change noticeably when spin−orbit coupling is considered. The ground spin-mixed state is $\Omega = 0^+$, which is quasidegenerate with $\Omega = 0^-$. The relative energies of the energy minima for the lowest $\Omega = 0^+$, 0^-, 1, 2, 3, and 4 states are 0, 0, 73, 149, 230, and 316 cm^{-1}. Since the spin−orbit splittings at the dissociation limit are

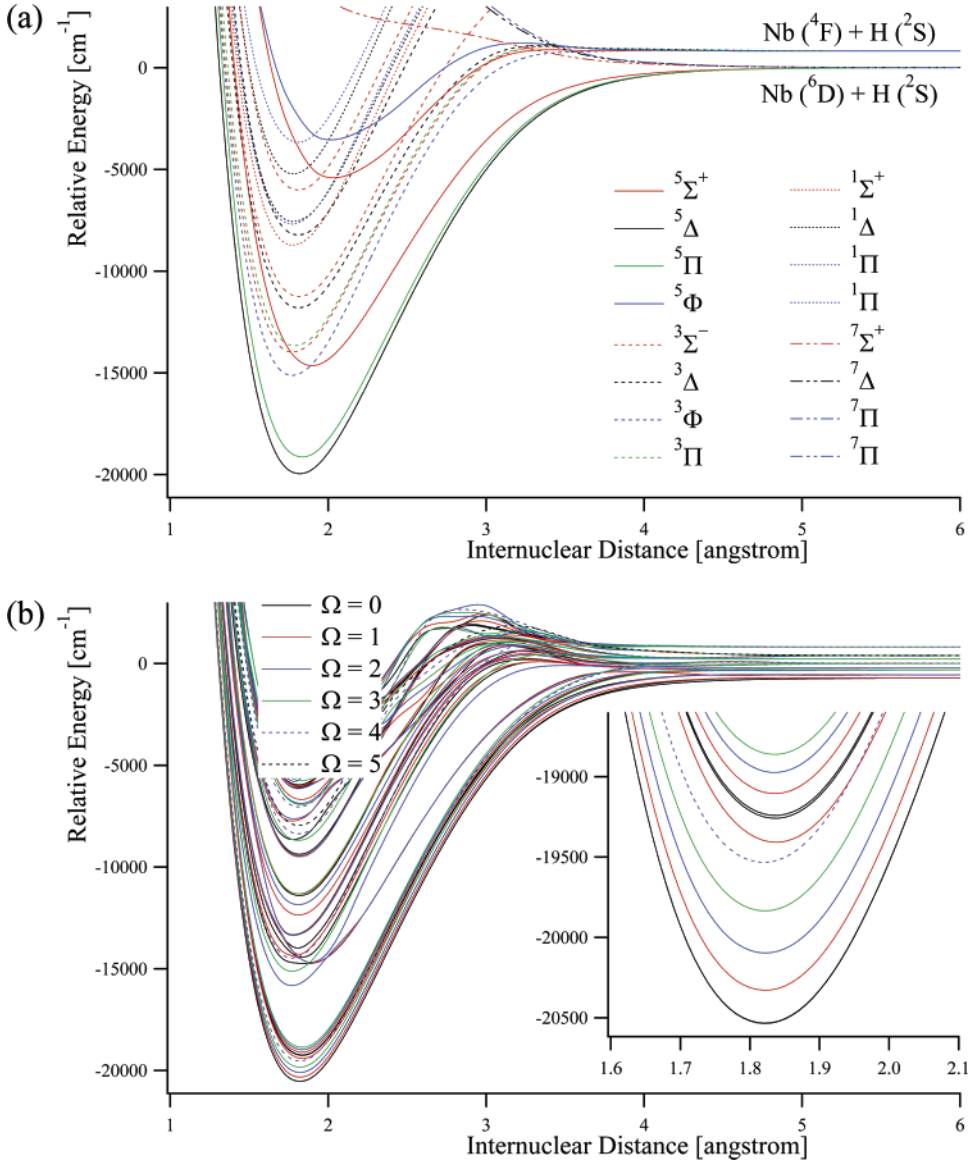

Figure 2. NbH potential energy curves obtained with use of quartet MCSCF+SOCI/SBKJC(f,p) wave functions, where the MCSCF active space includes two sets of 4d and 5s orbitals: (a) low-lying adiabatic states and (b) low-lying spin-mixed states. The inset figure is a close-up view near the energy minima.

somewhat larger than those at the equilibrium distance, D_e becomes slightly smaller when spin−orbit coupling is added (14923→14766 cm^{-1} for the $\Omega = 0^+$ state) (Table 1). The $\Omega = 0^+$, 0^-, 1, and 2 states correlate with the lowest (ground) spin-mixed state (V($^4F_{3/2}$) + H($^2S_{1/2}$)) in the dissociation limit, while the lowest $\Omega = 3$ and 4 states correlate with the second and third spin-mixed states ($^4F_{5/2}$ and $^4F_{7/2}$) of V.[48] Thus, the spin−orbit coupling effects in this molecule are mainly limited to a 157-cm^{-1} correction to the dissociation energy.

There are several theoretical and experimental reports on VH: the D_e is in the range of 13 000−23 000 cm^{-1}. The latest experimental investigations[49,75] report 17 173 and 17 181 cm^{-1} for the ground state D_e, so that our ECP (14 923 cm^{-1}) and AE (15 709 cm^{-1}) values are somewhat smaller. Our values of R_e (1.75−1.76 Å) are somewhat longer in comparison with some of those (1.68−1.74 Å) reported previously,[49−53] although our results agree quite well with the value of 1.74 Å obtained with a similar level of calculation by Walch et al.[51] The AE D_e values are somewhat closer to experiment and larger than the ECP values, while the R_e values are not very different.

3.2. Potential Energy Curves for NbH. If an active space represented by 4d5s5p(Nb)+1s(H) orbitals is used, then the dissociation limit is found to be ^{4}F(Nb)[(4d)^3(5s)^2]+^{2}S(H), but experimentally it is known that the ^{4}F state is the second lowest state and the ground state is ^{6}D [(4d)^4(5s)^1].[56] MCSCF+SOCI calculations performed separately for the ^{6}D and ^{4}F states result in the ^{6}D state being higher in energy than the ^{4}F state by 577 (ECP) and 1398 (AE) cm^{-1}. The orbital analyses in the present calculations suggest that the active 4dπ orbitals strongly interact with the virtual dπ orbitals rather than the active 5pπ orbitals. Therefore, we used an active space represented by the 4d5s5d6s-(Nb)+1s(H), and the MCSCF orbitals were optimized for the lowest $^5\Sigma^+$, $^5\Pi$, and $^5\Delta$ states, since these three states correlate with the Nb ^{6}D state in the dissociation limit. The external space for the SOCI calculations includes the orbitals corresponding to 5p6p(Nb)+2s2p(H) orbitals. This method is referred to as the "dsds" space in the following discussion. In the ECP calculations, the dsds active space provides the correct energetic order of the ^{6}D and ^{4}F states in Nb atom, though the energy gap between these states is smaller than the experimental

TABLE 2: Spectroscopic Parameters for the Low-Lying Adiabatic and Spin-Mixed States in NbH, Obtained with SOCI Based on the dsds MCSCF Active Space[a]

state	method	D_e	R_e	T_e	ω_e	$\omega_e x_e$	B_e	α_e	μ_e	refs
$^5\Delta$	ECP	19944	1.807	0	1611	22.39	5.110	0.203	2.5939	
	AE	21357	1.827	0	1576	19.41	5.053	0.185	2.4873	
$^5\Pi$	ECP	19102	1.818	842	1591	21.84	5.029	0.202		
	AE	21397	1.838	740	1558	16.70	4.982	0.182		
$^5\Sigma^+$	ECP	14653	1.909	5292	1487	28.98	4.705	0.203		
	AE	15434	1.933	7201	1401	20.95	4.520	0.179		
spin-mixed states										
$\Omega = 0^+$	ECP	19811	1.808	0	1607	22.25	5.102	0.202		
	AE	21741	1.829	0	1570	18.83	5.044	0.184		
$\Omega = 0^-$	ECP	19814	1.808	2	1607	22.24	5.102	0.202		
	AE	21743	1.829	1	1570	18.88	5.044	0.184		
$\Omega = 1$	ECP	19609	1.808	207	1605	22.24	5.099	0.202		
	AE	21573	1.829	169	1567	18.56	5.040	0.184		
$\Omega = 2$	ECP	19531	1.808	439	1605	22.25	5.099	0.203		
	AE	21383	1.829	364	1567	18.49	5.040	0.184		
$\Omega = 3$	ECP	19514	1.808	700	1606	22.31	5.102	0.203		
	AE	21533	1.828	589	1569	18.67	5.044	0.184		
$\Omega = 4$	ECP	19535	1.807	1000	1611	22.43	5.111	0.203		
	AE	21762	1.827	853	1576	19.39	5.055	0.186		
$^5\Delta$	RECP	20972	1.791		1583					53
	MCSCF+SOCI/RECP	21537	1.788		1725				2.29	58
	MCPF	20972	1.791		1583				2.452	58, 59
	CPF	21053	1.793		1573				2.484	59
	RECP	21537	1.787	0	1752				2.20	60
$^5\Pi$	RECP	20811	1.807	720	1742				2.64	60
$^5\Sigma^+$	(RECP)	(15648)	(1.821)	(7687)	(1572)				(3.77)	60
$^5\Phi$	(RECP)		(1.873)	(14823)	(1436)				(0.45)	60
$^5\Delta$	MCPF	21370	1.79							61

[a] See the footnote *a* for Table 1.

observation (the energy gap is calculated to be only 108 cm^{-1}). *In the AE method, though the energy gap between these states is reduced to 1126 cm^{-1} with the dsds active space, and the ^4F state is still lower in energy than the ^6D state.*

The ground state of NbH is $^5\Delta$ within the adiabatic scheme in both ECP and AE calculations. Figure 2 illustrates the potential energy curves obtained with the dsds active space followed by SOCI calculations.[57] Since the lowest ^6D and ^4F states of Nb are very close in energy, the spin−orbit interaction makes their spin states mix strongly with each other. At the dissociation limit the states corresponding to Nb atomic states are computed to be in the following order: $^6D_{1/2}$, $^6D_{3/2}$, $^6D_{5/2}$, $^4F_{3/2}$, $^6D_{7/2}$, $^4F_{5/2}$, $^6D_{9/2}$, $^4F_{7/2}$, and $^4F_{9/2}$; and their relative energies are 0, 154, 398, 493, 718, 936, 1102, 1523, and 2219 cm^{-1} in the ECP calculations. For the AE calculations the order is $^4F_{3/2}$ (−327), $^6D_{1/2}$ (0), $^4F_{5/2}$ (42), $^6D_{3/2}$ (128), $^6D_{5/2}$ (337), $^4F_{7/2}$ (493), $^6D_{7/2}$ (649), $^6D_{9/2}$ (868), and $^4F_{9/2}$ (1186). The spin−orbit splittings in each group of the ^6D or ^4F spin-mixed states are in good agreement with a previous report[26] and the experimental results.[56] The experimental separation of the energetic centers of the groups of states arising from spin−orbit splitting of the ^6D or ^4F terms is large enough to provide no overlap between the groups at the dissociation limit; however, some overlap is seen in our calculations for a wide range of internuclear distance, possibly causing the somewhat peculiar shape of the energy curves.

The potential energy curves of several low-lying spin-mixed states are plotted at the bottom of Figure 2. The AE results are very similar to these curves (Figure 2S). The ground (spin-mixed) state has $\Omega = 0^+$, and the lowest $\Omega = 0^-$ is nearly degenerate with this state. Although the lowest $^5\Pi$ state is close in energy to the lowest $^5\Delta$ within the adiabatic scheme, a rather weak spin−orbit interaction is observed between these states (see Table 4). As a result, the lowest $\Omega = 0^+$, 0^-, 1, 2, 3, and 4 states have more than 90% contributions from $^5\Delta$, and their R_e are approximately equal to those of the $^5\Delta$ state (1.808 Å in Table 2). As mentioned for VH, the spin−orbit splittings in the dissociation limit are slightly smaller than those near the energy minimum of the ground state, so that the D_e is slightly decreased (19944→19811 cm^{-1}) for $\Omega = 0^+$ by the spin−orbit coupling effects.

With the exception of the nearly degenerate state order in the dissociation limit, the energy curves with and without spin−orbit coupling in Figure 2 obtained with the dsds active space are very similar to those obtained with use of the 4d5s5p-(Nb)+1s(H) active space. The D_e, R_e, and ω_e in the ground spin-mixed state are larger than those obtained by using the 4d5s5p(Nb)+1s(H) active space by 900 cm^{-1}, +0.015 Å, and 20 cm^{-1}, respectively. The D_e values found in the literature are in the range of 20 900−21 600 cm^{-1} (see Table 2), in good agreement with our results, and our R_e value is 0.03−0.04 Å longer. However, there are no experimental values reported, to the best of our knowledge. Similar to VH, the AE values of D_e are somewhat larger than the ECP ones and the R_e are not very different.

3.3. Potential Energy Curves for TaH. As mentioned earlier, the ground state of TaH is consistently found to be a triplet, using both triplet and quintet state-averaged orbitals and for either ECP or AE basis sets. Therefore, all results below are based on MCSCF calculations state-averaging the lowest $^3\Sigma^-$, $^3\Delta$, $^3\Pi$, and $^3\Phi$ states. The potential energy curves obtained at the SOCI level of theory are plotted in Figure 3 (and Figure 3S). As depicted in these figures, the lowest $^3\Phi$ state is lower than the quintet states near the R_e within the adiabatic scheme.

In the ECP calculations, the lowest spin-mixed state is found to have $\Omega = 2$ after the inclusion of the spin−orbit coupling effect, using the MCSCF orbitals optimized for the triplet states. This state has more than 90% contribution from the $^3\Phi$ state. The second lowest spin-mixed state has $\Omega = 0^+$ character and consists of 43% $^3\Sigma^-$ and 43% $^3\Pi$ (see Table 4). The contribution of the $^5\Delta$ state is only 4% to this state. Strong spin−orbit coupling between the $^3\Sigma^-$ and $^3\Pi$ states leads to an energy gap

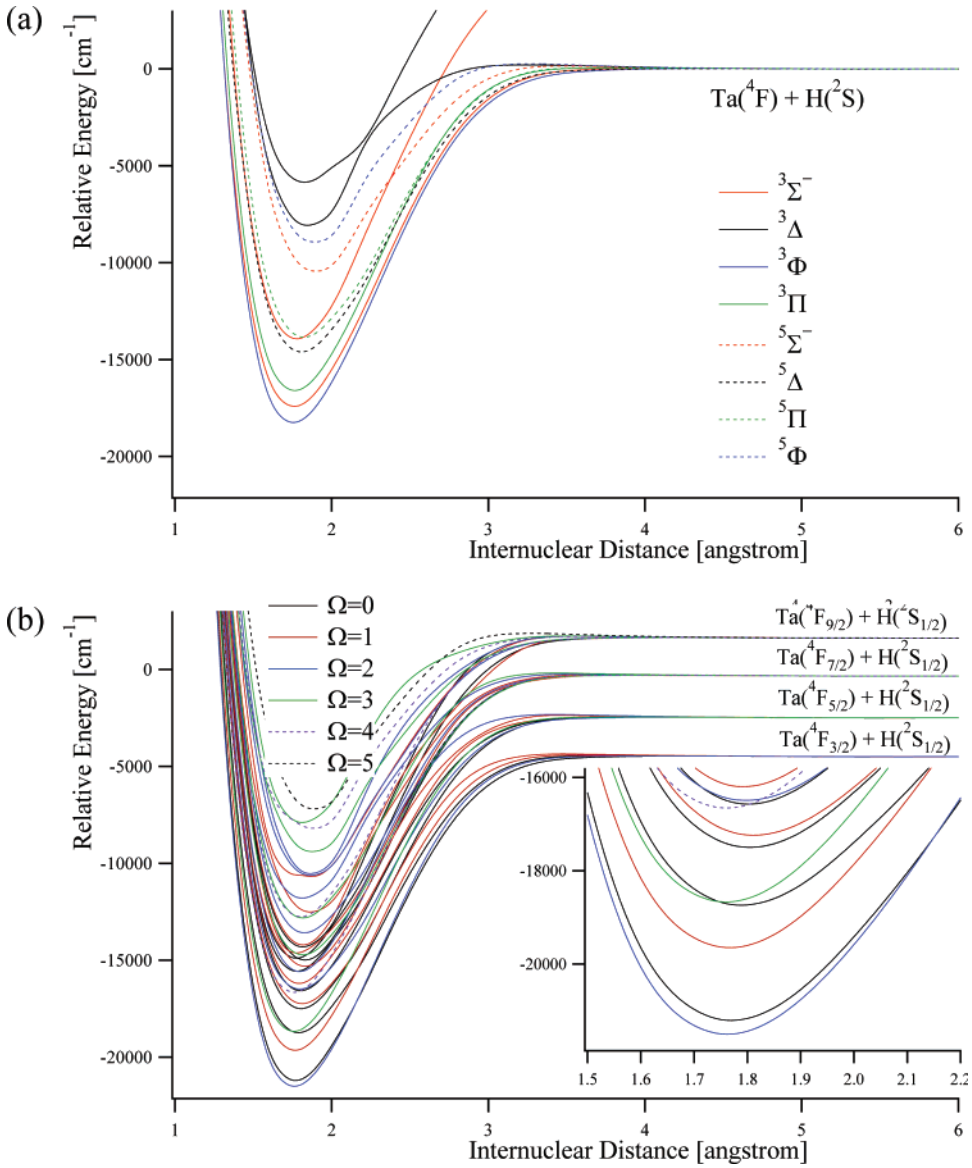

Figure 3. TaH potential energy curves obtained with use of triplet MCSCF+SOCI/SBKJC(f,p) wave functions: (a) low-lying adiabatic states and (b) low-lying spin-mixed states. The inset figure is a close-up view near the energy minima.

of only 314 cm^{-1} between the $\Omega = 0^+$ and 2 states at the energy minimum of the $\Omega = 2$ state, but the $\Omega = 2$ is still the lowest. The third state $\Omega = 1$ has 39% $^3\Sigma^-$ and 47% $^3\Pi$ contributions. The lowest $\Omega = 0^-$ is the fourth state and has a large contribution from the $^5\Delta$ state, but its principal contribution is provided by $^3\Pi$ (56%). The $\Omega = 0^+$ state generated by Λ-doubling of the $\Omega = 0$ in the $^5\Delta$ is the sixth, where the reverse energetic order of the $\Omega = 0^+$ and 0^- states is derived by strong spin−orbit couplings among states packed closely in energy. The AE results (Figure 3S) are similar to those of the ECP calculations, although the energy difference between the ground spin-mixed state ($\Omega = 2$) and the second state ($\Omega = 0^+$) for the former method is somewhat larger (581 cm^{-1} at the energy minimum of the $\Omega = 2$ state). Thus, we conclude that the $\Omega = 2$ state is the ground state in TaH at the level of theory employed here.

The ground spin-mixed state $\Omega = 2$ has $R_e = 1.762$ Å and $D_e = 17\,002$ cm^{-1}. Spin−orbit coupling effects make R_e longer by 0.006 Å and the D_e smaller by 1240 cm^{-1} (see Table 3). The second spin-mixed state $\Omega = 0^+$ has a somewhat longer R_e (1.770 Å) and a smaller D_e (16 705 cm^{-1}). The AE calculations have a larger D_e by 4300−4600 cm^{-1} and shorter R_e by about 0.04−0.05 Å for these two states compared with the ECP results. Although the ECP basis sets employed in the present study are not flexible enough to provide quantitative predictions, the present AE method given the basis set and the wave function type tends to overestimate D_e.

To our knowledge, there are no experimental reports on TaH. Cheng and Balasubramanian[62] have reported that the lowest $^3\Phi$ state is 2526 cm^{-1} lower in energy than the lowest $^5\Delta$ at the RECP level of theory. Including spin−orbit coupling, they predicted a ground state of $\Omega = 0^+$ originating from the $^5\Delta$ state, while the lowest $\Omega = 2$ state, originating from the $^3\Phi$ state, is only 326 cm^{-1} higher in energy than the $\Omega = 0^+$ state. Wittborn et al. reported that the ground state of TaH is $^3\Phi$ using the AE/PCI80 and AIMP/PCI80 methods,[63] but no comment is made on the spin-mixed state structure.

3.4. Potential Energy Curves in Group 3 Hydrides, ScH, YH, and LaH. The MIDI basis set has been optimized for the lowest ^{2}F state ([4f]^1 configuration) in atomic La; this state is computed to be the ground state, even when dynamic correlation effects are included, contrary to the experimental observation that ^{2}D is the ground state.[56] Therefore, AE calculations were

TABLE 3: Spectroscopic Parameters for the Low-Lying Adiabatic and Spin-Mixed States in TaH, Where the MCSCF Orbitals Are Optimized for the Lowest $^3\Sigma$, $^3\Pi$, $^3\Delta$, and $^3\Phi$ States[a]

state	method	D_e	R_e	T_e	ω_e	$\omega_e x_e$	B_e	α_e	μ_e	refs
$^3\Phi$	ECP	18242	1.756	0	1776	26.84	5.442	0.224	1.0369	
	AE	22636	1.706	0	1672	6.68	5.726	0.208	1.1891	
$^3\Sigma^-$	ECP	17409	1.762	833	1728	25.74	5.402	0.222		
	AE	21703	1.721	934	1600	4.14	5.645	0.200		
$^3\Pi$	ECP	16592	1.765	1649	1748	26.67	5.387	0.224		
	AE	20691	1.721	1946	1635	6.27	5.641	0.205		
$^3\Delta$	ECP	8070	1.844	10171	1845	80.14	5.239	0.358		
	AE	12325	1.793	10312	1470	17.48	5.278	0.230		
$^5\Delta$	ECP	14601	1.807	3640	1589	24.21	5.109	0.218		
	AE	19841	1.778	2796	1536	6.76	5.332	0.187		
spin-mixed states										
$\Omega = 2$	ECP	17002	1.762	0	1751	25.90	5.403	0.223		
	AE	21644	1.711	0	1655	6.71	5.696	0.208		
$\Omega = 0^+$	ECP	16705	1.770	298	1728	28.03	5.355	0.226		
	AE	21075	1.729	569	1607	6.67	5.594	0.204		
$\Omega = 1$	ECP	15146	1.767	1856	1721	28.98	5.378	0.233		
	AE	19720	1.725	1924	1594	11.59	5.623	0.222		
$\Omega = 0^-$	ECP	14237	1.788	2765	1602	26.01	5.217	0.231		
	AE	19137	1.766	2507	1485	4.18	5.393	0.199		
$\Omega = 3$	ECP	16173	1.760	2834	1758	28.68	5.420	0.230		
	AE	20899	1.711	2329	1652	9.33	5.701	0.216		
$\Omega = 0^+$	ECP	15001	1.805	4005	1587	22.76	5.128	0.212		
	AE	19901	1.779	3327	1526	4.90	5.331	0.179		
$\Omega = 1$	ECP	12737	1.812	4266	1543	20.31	5.097	0.213		
	AE	18075	1.790	3569	1501	3.88	5.284	0.173		
$\Omega = 4$	ECP	16317	1.761	4848	1749	29.37	5.410	0.232		
	AE	20933	1.715	4121	1630	8.64	5.672	0.215		
$\Omega = 2$	ECP	13994	1.797	5012	1534	20.46	5.163	0.227		
	AE	18994	1.790	4234	1465	3.91	5.294	0.183		
$^3\Phi$	RECP	19278	1.749	0	1812				2.00	62
$^3\Sigma^-$	RECP	18310	1.747	1000	1837				1.97	62
$^3\Pi$	RECP	17665	1.756	1620	1795				1.94	62
$^3\Delta$	RECP	7905	1.796	11370	1647				2.75	62
$^5\Delta$	RECP	16778 (20246)	1.785	2526	1741				2.08	62
$\Omega = 0^+$	RECP		1.775	0	1851					62
$\Omega = 2$	RECP		1.750	326	2133					62
$\Omega = 0^-$	RECP		1.789	1079	1841					62
$^3\Phi$	AE/PCI80	22741	1.762							63
	AIMP/PCI80	21678	1.757							63
	CASSCF	15319	1.77		1730					76
	ACPF-ds	19831	1.75		1800					76

[a] See the footnote *a* for Table 1.

not performed for LaH in the present investigation, since the spin−orbit calculations are not likely to provide meaningful results.

The ground state is calculated to be $^1\Sigma^+$ in all three hydrides within the ECP adiabatic scheme. After the inclusion of the spin−orbit coupling effects (Figure 4), the ground state has $\Omega = 0^+$ originating principally from the $^1\Sigma^+$ state; the contributions are computed to be 99.98% (ScH), 99.97% (YH), and 99.48% (LaH), respectively. Therefore, no important spin−orbit effect is observed in the ground state. Table 5 lists several spectroscopic parameters calculated for their ground states. The table also includes experimental and calculated results reported previously.[65,68,69] As described for the Group 5 hydrides, the ECP method generally provides somewhat smaller D_e values compared to the AE values. The calculated D_e for ScH is in surprisingly good agreement with the experimental value.[78] Our R_e values are slightly longer than the MCPF and AIMP results, and 0.01−0.03 Å longer than the experimental observations (see Table 5).

3.5. Periodic Trends. Figure 5 plots R_e and D_e for the Groups 3 and 5 hydrides, using the ECP method against the periodic row, together with those for the Group 4 hydrides reported previously.[28] Among the many general factors affecting the

TABLE 4: Percentage of Adiabatic States in Low-Lying Spin-Mixed States Obtained by the ECP Method at the Internuclear Separation *R* [angstroms]

mol.	Ω	components
VH	0^+	$^5\Delta$ (99.6%)
$R = 1.758$	0^-	$^5\Delta$ (99.6%)
	1	$^5\Delta$ (99.5%)
	2	$^5\Delta$ (99.4%)
	3	$^5\Delta$ (99.6%)
	4	$^5\Delta$ (100%)
NbH	0^+	$^5\Delta$ (94.7%), $^5\Pi$ (4.8%)
$R = 1.808$	0^-	$^5\Delta$ (94.9%), $^5\Pi$ (4.6%)
	1	$^5\Delta$ (92.1%), $^5\Pi$ (7.4%)
	2	$^5\Delta$ (91.3%), $^5\Pi$ (8.3%)
	3	$^5\Delta$ (92.8%), $^5\Pi$ (6.7%)
	4	$^5\Delta$ (99.3%)
TaH	2	$^3\Phi$ (93.3%), $^5\Delta$ (4.3%)
$R = 1.762$	0^+	$^3\Sigma$ (43.1%), $^3\Pi$ (43.1%), $^5\Delta$ (4.3%), $^1\Sigma$ (3.2%)
	1	$^3\Pi$ (47.0%), $^3\Sigma$ (39.3%), $^1\Pi$ (4.9%), $^5\Delta$ (3.9%)
	0^-	$^3\Pi$ (55.7%), $^5\Delta$ (33.7%), $^5\Pi$ (8.2%)
	3	$^3\Phi$ (93.7%), $^5\Delta$ (4.3%)
	0^+	$^5\Delta$ (60.8%), $^3\Sigma$ (18.0%), $^5\Pi$ (10.3%), $^1\Sigma$ (4.6%), $^3\Pi$ (2.4%)
	1	$^5\Delta$ (38.6%), $^3\Sigma$ (28.6%), $^5\Pi$ (16.6%), $^1\Pi$ (3.0%), $^3\Pi$ (2.6%)
	4	$^3\Phi$ (84.2%), $^5\Delta$ (10.9%), $^1\Gamma$ (3.7%)
	2	$^3\Pi$ (51.7%), $^5\Delta$ (29.5%), $^5\Pi$ (14.4%)

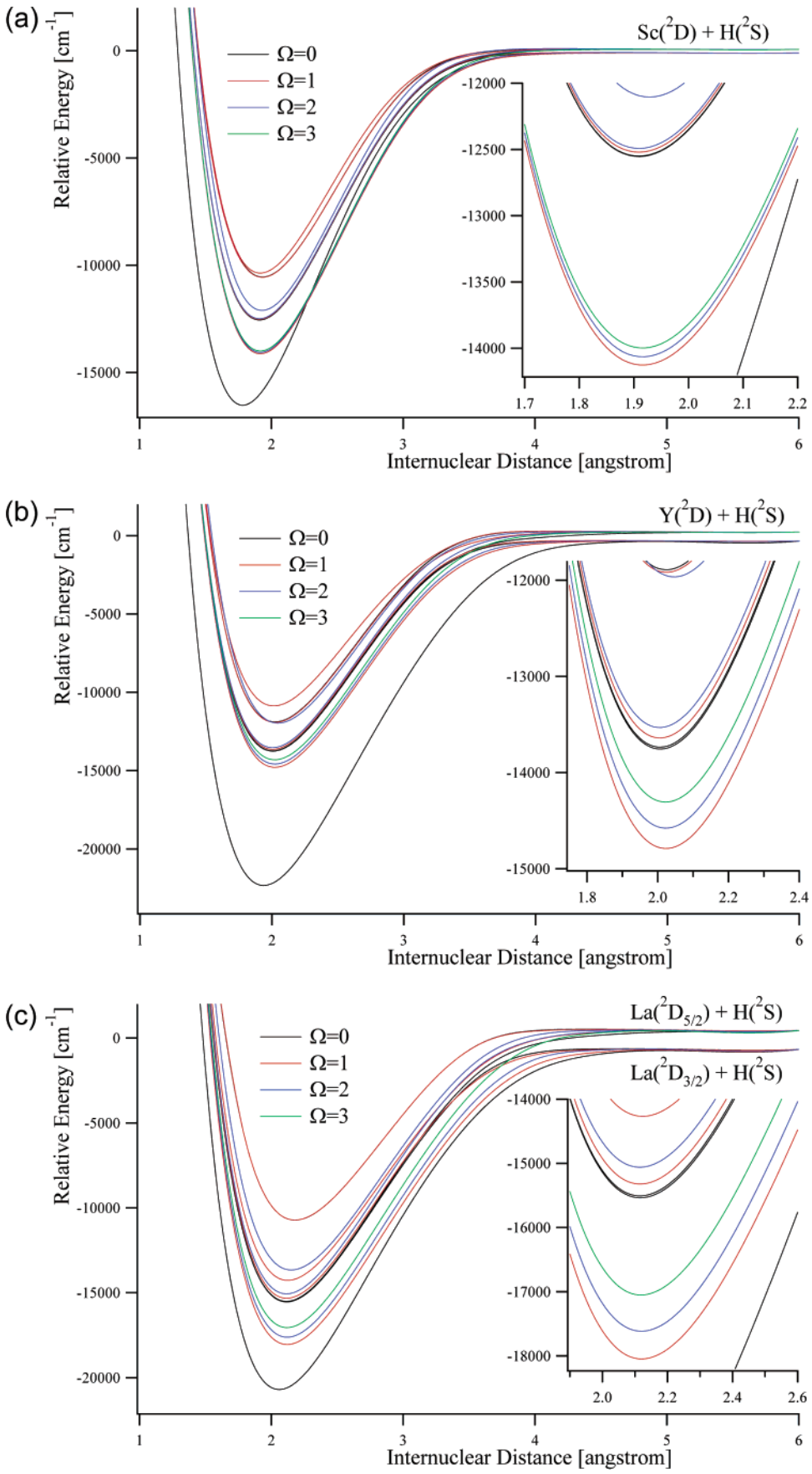

Figure 4. Potential energy curves of low-lying spin-mixed states obtained with use of singlet MCSCF+SOCI/SBKJC(f,p) wave functions: (a) ScH, (b) YH, and (c) LaH. The inset figures are close-up views near the energy minima.

periodic trends in the transition metal hydrides one can identify the following:

(a) An increase in the screening of the atomic charge by the inner shell electrons is observed as their number increases. This

TABLE 5: Spectroscopic Parameters in the Ground States of ScH, YH, and LaH[a]

state	method	D_e	R_e	ω_e	$\omega_e x_e$	B_e	α_e	μ_e	refs
ScH									
$^1\Sigma^+$	ECP	16525	1.782	1564	26.31	5.364	0.226	1.3337	
	AE	21440	1.798	1549	15.80	5.281	0.187	1.0801	
$\Omega = 0$	ECP	16428	1.782	1564	26.34	5.364	0.226		
	AE	21365	1.798	1550	15.81	5.281	0.187		
	B3LYP	14060	1.730	1663					49
	PKP	10567	1.85	1173	30.7	4.9	0.19		50
	MCPF	18292	1.776	1587					52, 77
	MRD-CI	18552	1.804	1621					64
	B3LYP		1.731−1.759	1584−1677					67
	MP2		1.764	1668					79
	full CI	16294	1.767	1627					80
	expt		1.775	1547					65
	expt	16613 ± 700							78
	expt			1530					79
YH									
$^1\Sigma^+$	ECP	22322	1.937	1497	21.11	4.486	0.166	1.3338	
	AE	25413	1.938	1491	16.95	4.490	0.154	1.2317	
$\Omega = 0$	ECP	21984	1.937	1497	21.11	4.486	0.166		
	AE	25128	1.938	1491	16.96	4.490	0.154		
		23634							
	SOCI		1.954	1522				1.28	58
	(24199)								
	MCPF	23795	1.961	1559				1.535	58, 59, 61
	CPF	23975	1.961	1558				1.556	59
	RECP	24602	1.865	1510					66
	MP2		1.918	1566					79
	expt		1.923	1530	19.44	4.576	0.091		68
	expt							1.569	73
	expt			1470−1489					79
LaH									
$^1\Sigma^+$	ECP	20663	2.060	1429	20.93	3.957	0.143	2.244	
$\Omega = 0$	ECP	20026	2.060	1428	21.02	3.956	0.144		
	AE/PC180	23888	2.074						63
	AIMP	23745	2.080						63
	MP2		1.996	1480					70
	MP2		2.006	1500					70
$^1\Sigma^+$	CASSCF	21580	2.11	1350					76
	ACPF-ds	22105	2.08	1380					76
	MP2		2.045	1448					79
	MCSCF	20972	2.08	1433				2.42	81
	DFT	24118	2.08	1378				2.82	82
		24521	1.998	1521					
	MRACPF								
		22747	2.037	1488					83
	ZORA	30006	2.005	1416					84
	DKH	30006	2.004	1419					84
	CCSD(T)	23311	2.028	1447					85
	B3LYP	23473	2.006	1461					85
	expt		2.032			4.081	0.077		69
	expt			1344					79

[a] See the footnote *a* for Table 1.

in general leads to weaker bonding, as found for the main group elements as well.

(b) Relativistic contraction of s and expansion of d orbitals is observed.[71] This leads to stronger bonding involving s electrons and weaker bonding for d electrons.

(c) Additional screening due to the filled f-subshell that appears in Hf and Ta is seen, but f-subshells are empty and fairly inactive for other elements considered here.

(d) Spin−orbit coupling of the ground atomic states is very different and it grows both vertically and horizontally. For example, the splitting[56] in La is 1053 cm^{-1}, in Hf 4568 cm^{-1}, and in Ta 5621 cm^{-1}, which in part comes from increased multiplicity (2, 3, and 4 for La, Hf, and Ta, respectively). The total spin−orbit effect on D_e (that is, the value with and without the interaction) is fairly small for all compounds. However, this is misleading, especially for HfH and TaH, as the SOC interaction splits atomic and mixes molecular levels in a complicated way. Indeed, one can see that the Ω levels of $^3\Phi$ in TaH span 4848 (ECP) or 4121 (AE) cm^{-1} (Table 3).

(e) The complicated structure of the states arises from the partially filled d orbitals and results in near degeneracies in energy levels that are not simply related to the group or position in the row. This is explicitly seen, for example, in the different atomic ground states within the same group (Nb has a ^{6}D ground state, whereas the ground states of V and Ta are ^{4}F).

While it can be generally expected that an increase in the equilibrium distances corresponds to a decrease in the dissociation energy as can be seen by comparing YH and LaH, it is somewhat surprising to observe that both D_e and R_e decrease when going from HfH to TaH. Spin−orbit coupling interactions that differ at the equilibrium vs the dissociation limit may be the reason.

3.6. Emission Spectra. Ram and Bernath have reported spectral analyses on ScH, YH, and LaH.[65,68,69] Recently, Jakubek

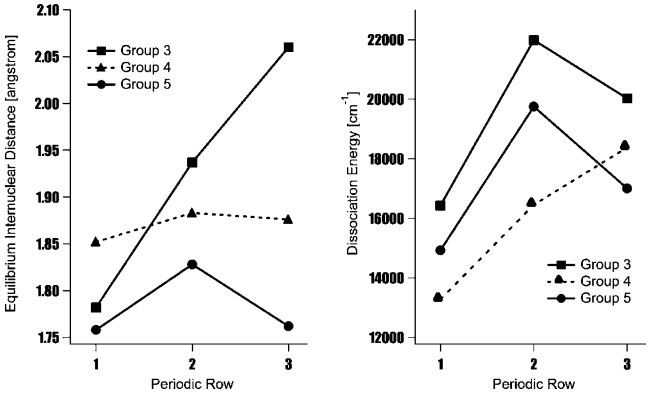

Figure 5. Periodic trends for the equilibrium internuclear distances R_e [angstrom] and dissociation energies D_e [cm^{-1}]: Group 3, squares connected by solid lines; Group 4, triangles connected by broken lines; and Group 5, circles connected by solid lines.

et al. have reexamined experimentally YH[72,73] and LaH[74] in more detail. In this section, ECP results for transitions among the spin-mixed states in Group 3 hydrides will be discussed in comparison with the experimental observations.

Ram and Bernath[65] observed 0−0 band origins at 5 404, 13 574, and 20 547 cm^{-1} for ScH and assigned them as the $B^1\Pi-X^1\Sigma^+$, $C^1\Sigma^+-X^1\Sigma^+$, and $G^1\Pi-X^1\Sigma^+$ emissions, respectively. As suggested by Anglada et al.,[64] a small moment (μ_{TM} = 0.42 au) is obtained for the transition between the ground state and the $B^1\Pi$ state, although a rather strong emission is observed for the transition between these states by Ram and Bernath.[65] According to our results, large moments are obtained for the transitions between the ground state ($X^1\Sigma^+$) and $C^1\Sigma^+$/$D^1\Pi$ states in ScH. Within an adiabatic scheme, the 0−0 band origin of the $B^1\Pi-X^1\Sigma^+$ transition is computed to be 6028 cm^{-1}. If spin−orbit coupling is considered, this transition corresponds to that between the lowest $\Omega = 0^+$ and the fourth $\Omega = 1$ states; it is calculated to have a 0−0 origin of 5829 cm^{-1} (6525 cm^{-1} for the vertical excitation; see Table 6). This estimate is about 9% larger than the experimental result (5404 cm^{-1}). Furthermore, the 1−1, 1−0, and 2−1 origins are calculated to be 5829, 7073, and 8273 cm^{-1}, respectively. The corresponding experimental values are 5220, 6767, and 6536 cm^{-1}, so the errors are less than 10%. The $C^1\Sigma^+-X^1\Sigma^+$ transition corresponds to the transition from the fifth $\Omega = 0^+$ state to the lowest $\Omega = 0^+$ state if spin−orbit coupling is included, and our calculation overestimates its 0−0 and 1−1 origins (15 149 and 16 713 cm^{-1}) by about 12%. Such overestimation may be caused by the fact that the electron correlation effects are underestimated for the higher state at the level of theory used here.

The transition energy from the $G^1\Pi$ state to the ground state was also reported by Ram and Bernath. Our study assigns a large moment (μ_{TM} = 0.96 au) to the corresponding $^1\Pi-X^1\Sigma^+$ transition and good estimation of the transition energy (about 12% overestimation). However, the lowest $^1\Phi$ state is found to be lower in energy than this $^1\Pi$ state, i.e., the present study assigns these states as $G^1\Phi$ and $H^1\Pi$. Our calculations also suggest that the $D^1\Pi-X^1\Sigma^+$ transition has a rather large moment (μ_{TM} = 2.88 au) and has a 0−0 transition energy of 17 302 cm^{-1} (17 484 cm^{-1} vertical). Unfortunately, this transition is not referred to in the experimental paper.[65]

In YH, the experimental energy difference between the ground state ($X^1\Sigma^+$) and the lowest triplet state ($a^3\Delta$) has been reported as 6900 cm^{-1} by Ram and Bernath,[68] but smaller differences were obtained by Jakubek et al.[72] as shown in Table 6. Our calculations provide 0−0 transition energies of 7461, 7672, and 7944 cm^{-1} from the ground state ($\Omega = 0^+$) to the Ω = 1, 2, and 3 states, respectively, whose main configuration is the $a^3\Delta$ state. Accordingly, our calculations overestimate them by about 20%, even though good agreement is obtained for the transitions from the $C^1\Sigma^+$ ($\Omega = 0^+$, μ_{TM} = 1.50 au). The transition energy to the $D^1\Pi$ ($\Omega = 1$, μ_{TM} = 4.08 au) state is about 20% larger than the experimental value. Moreover, the emission spectra to the lowest triplet state ($a^3\Delta$) were reported by Ram and Bernath[68] and Jakubek et al.[72] The band origins were experimentally found at the transition energies of 11 378, 11 499, and 11 584 cm^{-1} and were assigned as $^3\Phi_2-^3\Delta_1$, $^3\Phi_3-^3\Delta_2$, and $^3\Phi_4-^3\Delta_3$ subbands of the $e^3\Phi-a^3\Delta$ transition. Our estimates of the origins of these transitions are 11 989, 12 059, and 12 078 cm^{-1} (μ_{TM} = 5.32 au), respectively. These origins are overestimated by less than 5%, so that our results are nearly quantitative. We also find that the emission of the $f^3\Delta-a^3\Delta$ transition (12 900−13 000 cm^{-1}) is energetically close to the $e^3\Phi-a^3\Delta$ transition and that its transition moment is also large (μ_{TM} = 2.62 au). However, Jakubek et al.[72] assigned this as the $f^3\Pi-a^3\Delta$ transition.

For LaH, we find strong emission in the transition-energy range of 15 000−20 000 cm^{-1}. Even though the emissions can be assigned as a transition from $^1\Sigma^+$ or $^1\Pi$ to the ground state ($X^1\Sigma^+$), it is difficult to determine which peaks correspond to the transitions from some specific states in the adiabatic scheme because of strong spin−orbit mixing. The lowest excited singlet state is $^1\Pi$ in this molecule, although it is $^1\Delta$ in ScH and YH. Ram and Bernath[69] reported that the 0−0 and 1−1 emissions from $A^1\Pi$ to the ground state appear at a transition energy of

TABLE 6: Transition Energies [cm^{-1}] and Transition Moments [au] for Emission Spectra in Group 3 Hydrides Obtained with Use of MCSCF+SOCI/SBKJC(f,p) Wave Functions

emission		vibrational	transition energy		error	transition
from	to	states	expt[a]	present	[%]	moment
ScH						
$B^1\Pi_1$	$X^1\Sigma_0^+$	0−0	5404	5829	8	0.42
		1−1	5220	5829	12	
		1−0	6767	7073	5	
		2−1	6536	8273	27	
$C^1\Sigma_0^+$	$X^1\Sigma_0^+$	0−0	13574	15149	12	1.32
		1−1		16713		
$D^1\Pi_1$	$X^1\Sigma_0^+$	0−0		17302		2.88
$G^1\Pi_1$	$X^1\Sigma_0^+$	0−0	20547	22556	12	0.96
YH						
$a^3\Delta_1$	$X^1\Sigma_0^+$	0−0	6205	7461	20	
$a^3\Delta_2$	$X^1\Sigma_0^+$	0−0	6368	7672	20	
$a^3\Delta_3$	$X^1\Sigma_0^+$	0−0	6562	7944	21	
$C^1\Sigma_0^+$	$X^1\Sigma_0^+$	0−0	14295	15258	7	1.50
$D^1\Pi_1$	$X^1\Sigma_0^+$	0−0	15756	19119	21	4.08
$e^3\Phi_2$	$a^3\Delta_1$	0−0	11378	11989	5	5.32
$e^3\Phi_3$	$a^3\Delta_2$	0−0	11499	12059	5	5.32
$e^3\Phi_4$	$a^3\Delta_3$	0−0	11584	12078	4	5.32
$f^3\Delta_1$	$a^3\Delta_1$	0−0		12815		2.62
$f^3\Delta_2$	$a^3\Delta_2$	0−0		12810		2.62
$f^3\Delta_3$	$a^3\Delta_3$	0−0		12849		2.82
LaH						
$A^1\Pi_1$	$X^1\Sigma_0^+$	0−0	4534	6354	40	1.08
		1−1	4430	6202	40	
$C^1\Sigma_0^+$	$X^1\Sigma_0^+$	0−0	10151	11323	12	1.27
$D^1\Pi_1$	$X^1\Sigma_0^+$	0−0		15396		2.88
$I^1\Pi_1$	$X^1\Sigma_0^+$	0−0		18033		3.16
$d^3\Phi_2$	$a^3\Delta_1$	0−0	5956	7365	24	3.48
$d^3\Phi_3$	$a^3\Delta_2$	0−0	6238	7582	22	3.48
$d^3\Phi_4$	$a^3\Delta_3$	0−0	6307	7637	21	3.48
$e^3\Sigma_{0^+}^-$	$a^3\Delta_1$	0−0		7906		0.64
$e^3\Sigma_1^-$	$a^3\Delta_1$	0−0		8388		0.30
$e^3\Sigma_1^-$	$a^3\Delta_2$	0−0		7957		1.32

[a] See refs 65 (ScH), 72 (YH), and 69 and 75 (LaH).

TABLE 7: Predicted Transition Energies [cm^{-1}] and Transition Moments [au] for 0−0 Emission Spectra in Group 5 Hydrides Obtained with Use of MCSCF+SOCI/SBKJC(f,p) Wave Functions

emission		transition	transition
from	to	energy	moment
VH			
$F^5\Delta_{0^+}$	$X^5\Delta_{0^+}$	15048	0.74
$F^5\Delta_{0^-}$	$X^5\Delta_{0^-}$	15048	0.74
$F^5\Delta_1$	$X^5\Delta_1$	15018	1.46
$F^5\Delta_2$	$X^5\Delta_2$	15006	1.46
$F^5\Delta_3$	$X^5\Delta_3$	15451	1.46
$F^5\Delta_4$	$X^5\Delta_4$	15604	1.48
$C^5\Phi_1$	$X^5\Delta_{0^+}$	4717	0.32
$C^5\Phi_1$	$X^5\Delta_{0^-}$	4717	0.32
$C^5\Phi_2$	$X^5\Delta_1$	4765	0.64
$C^5\Phi_3$	$X^5\Delta_2$	4807	0.64
$C^5\Phi_4$	$X^5\Delta_3$	4843	0.64
$C^5\Phi_5$	$X^5\Delta_4$	4872	0.64
NbH			
$a^3\Phi_2$	$X^5\Delta_{0^+}$	4742	
$a^3\Phi_3$	$X^5\Delta_{0^+}$	5461	
$a^3\Phi_4$	$X^5\Delta_{0^+}$	6111	
$g^3\Gamma_3$	$a^3\Phi_2$	7103	0.50
$g^3\Gamma_4$	$a^3\Phi_3$	7111	0.47
$g^3\Gamma_5$	$a^3\Phi_4$	6474	0.45
TaH			
$D^3\Delta_1$	$X^3\Phi_2$	11744	0.40
$D^3\Delta_2$	$X^3\Phi_2$	12677	0.14
$D^3\Delta_3$	$X^3\Phi_2$	15354	0.20
$F^3\Delta_1$	$X^3\Phi_2$	12914	0.52
$F^3\Delta_2$	$X^3\Phi_2$	15024	0.05
$F^3\Delta_3$	$X^3\Phi_2$	16784	0.06
$C^3\Sigma_{0^+}$	0^+	6085	0.19
$C^3\Sigma_1$	0^+	6541	0.17
$?^5\Phi_1$	0^+	8602	0.22
$e^5\Pi_{0^+}$	0^+	14942	0.26
$e^5\Pi_1$	0^+	14480	0.07
$G^3\Pi_{0^+}$	0^+	17386	0.17
$G^3\Pi_1$	0^+	15788	0.12

4534 and 4430 cm^{-1}, respectively. Our estimates are 6354 and 6202 cm^{-1} (40% overestimation) and the transition moment is calculated to be 1.08 au for both transitions, while the emission energy from $C^1\Sigma^+$ ($\Omega = 0^+$, $\mu_{TM} = 1.27$ au) is in better agreement with that reported by Bernard et al.[74] (see Table 6). Their transition moments are smaller than that for the other strong emissions assigned as transitions from higher $^1\Pi$ states to the ground state. Emissions to the lowest triplet state ($a^3\Delta$) also appear at energies of 7365 ($^3\Phi_2-{}^3\Delta_1$), 7582 ($^3\Phi_3-{}^3\Delta_2$), and 7637 ($^3\Phi_4-{}^3\Delta_3$) cm^{-1} ($\mu_{TM} = 3.48$ au). These are assigned as the transitions from $d^3\Phi$, which is consistent with the corresponding observations (5956, 6238, and 6307 cm^{-1} for $^3\Phi_2-{}^3\Delta_1$, $^3\Phi_3-{}^3\Delta_2$, and $^3\Phi_4-{}^3\Delta_3$), though the transition energy is overestimated by about 21−24%. Additionally, the $e^3\Sigma^- - a^3\Delta$ transition is predicted to be observed in the same energetic range as the $d^3\Phi-a^3\Delta$.

Thus, it can be concluded that the present estimation is qualitatively reasonable, even though transition energies are overestimated by about 10% in the first- and second-row hydrides and 20−25% in the third-row hydride (see Table 6). In the following discussion, an attempt is made to predict some peak positions of strong emission spectra in Group 5 hydrides, since no experimental report on emission spectra is yet available for these hydrides.

As shown in Table 7, the largest moment ($\mu_{TM} = 1.48$ au) in VH is obtained at a transition energy of 15 599−15 620 cm^{-1} (15 006−15 604 cm^{-1} for the 0−0 transition). This is assigned to an $F^5\Delta-X^5\Delta$ transition in the adiabatic scheme. In the relativistic scheme, this transition has contributions from the $F^5\Delta_{0^+}-X^5\Delta_{0^+}$, $F^5\Delta_{0^-}-X^5\Delta_{0^-}$, $F^5\Delta_1-X^5\Delta_1$, $F^5\Delta_2-X^5\Delta_2$, $F^5\Delta_3-X^5\Delta_3$, and $F^5\Delta_4-X^5\Delta_4$ transitions. The lowest excited quintet state is $A^5\Pi$, but the moment for the $A^5\Pi-X^5\Delta$ transition is negligibly small. The $B^5\Sigma^- - X^5\Delta$ transition is symmetry forbidden, while the $C^5\Phi-X^5\Delta$ transition has a large moment ($\mu_{TM} = 0.64$ au), and its 0−0 origin is calculated to be 4717 ($C^5\Phi_1-X^5\Delta_{0^+}$ and $C^5\Phi_1-X^5\Delta_{0^-}$), 4765 ($C^5\Phi_2-X^5\Delta_1$), 4807 ($C^5\Phi_3-X^5\Delta_2$), 4843 ($C^5\Phi_4-X^5\Delta_3$), and 4872 ($C^5\Phi_5-X^5\Delta_4$) cm^{-1}, respectively. The $D^5\Pi-X^5\Delta$ transition also could be observed at a transition energy of 12 800−13 000 cm^{-1}, where the present prediction of the transition energy should be considered to have an error of about 10%.

It would be difficult to observe an emission spectrum for NbH, since only small moments are obtained for the transitions in the energetic range below 15 000 cm^{-1}. Strong emission is predicted to appear in the energetic range of 20 000−25 000 cm^{-1}, from the overlap of several $^5\Pi-X^5\Delta$, $^5\Delta-X^5\Delta$, and $^5\Phi-X^5\Delta$ transitions. The lowest triplet state is $^3\Phi$, and the 0−0 gap between $X^5\Delta$ and $a^3\Phi$ is calculated to be 4742 ($X^5\Delta_{0^+}-a^3\Phi_2$), 5461 ($X^5\Delta_{0^+}-a^3\Phi_3$), and 6111 ($X^5\Delta_{0^+}-a^3\Phi_4$) cm^{-1}. Emission spectra may be observed from $g^3\Gamma$ to this lowest triplet state. The transition moment is calculated to be 0.48 au and the 0−0 transition energies are predicted to be 7103 ($g^3\Gamma_3-a^3\Phi_2$), 6711 ($g^3\Gamma_4-a^3\Phi_3$), and 6474 ($g^3\Gamma_5-a^3\Phi_4$) cm^{-1}, where the excitation energies may be overestimated by more than 10%.

Because of strong spin−orbit coupling in TaH, it is difficult to determine which spin-mixed states should belong to a particular adiabatic state. Additionally, as described in the previous section, the ground state ($\Omega = 2$, $X^3\Phi_2$) and the next lowest state ($\Omega = 0^+$, mixture of $A^3\Sigma_{0^+}$ and $B^3\Pi_{0^+}$) are very close to each other in energy. Such conditions cause rather complicated spectra in TaH. Large moments are obtained for the transitions from the $D^3\Delta_1$ and $F^3\Delta_1$ states to the ground-state $X^3\Phi_2$ (Table 7). Their 0−0 transition energies are calculated to be 11 744 ($D^3\Delta_1-X^3\Phi_2$) and 12 914 ($F^3\Delta_1-X^3\Phi_2$) cm^{-1}, respectively. The $D^3\Delta_1$ state mixes strongly with $^3\Pi_1$ and $^5\Phi_1$, while $F^3\Delta_1$ interacts mildly with $^1\Pi_1$, $^3\Pi_1$, and $^5\Pi_1$. On the other hand, larger moments are obtained for transitions to the next lowest state ($\Omega = 0^+$) from $C^3\Sigma_{0^+}$ and from the combination of $G^3\Pi_{0^+}$ and $e^5\Pi_{0^+}$. These emissions are predicted to appear at the 0−0 transition energies of 6 085 and 14 942 cm^{-1}, respectively. Nevertheless, it would be quite difficult to recognize which emission peaks correspond to specific transitions because of strong spin−orbit coupling effects in this molecule.

4. Summary

The dissociation energy curves of low-lying spin-mixed states have been presented for Groups 3 and 5 hydrides with use of both ECP and AE approaches. The present paper reports a comprehensive set of theoretical results including dissociation energies (D_e), internuclear distances (R_e), electronic transition energies (T_e), harmonic frequencies (ω_e), anharmonicities ($\omega_e x_e$), and rotational constants (B_e and α_e). On the basis of the comparison with the corresponding AE results, we can conclude that the ECP approach is qualitatively accurate (sometimes semiquantitatively accurate) and can be applied in the studies of large molecular systems.

Transition energies and moments are also estimated between the spin-mixed states in these hydrides. The results for Group 3 hydrides were compared with the emission spectra reported by Ram and Bernath, and it is found that the transition energies are in qualitatively good agreement with the experimental observations. Especially in ScH and YH, the discrepancy is only

about 10%. On the basis of good agreement in Group 3 hydrides, the peak positions of strong emission are predicted in Group 5 hydrides. We hope that the present prediction is helpful in experimental trials on emission spectra for Group 5 hydrides and provide some encouragement for the applications of the simple ECP method to large molecular systems.

Acknowledgment. Financial support from a grant-in-aid for Scientific Research (Nos. 11166231, 12042237, and 14077215) from the Ministry in Education, Science, Sports, and Culture, Japan (to S.K.) is acknowledged, as is support of M.S.G. and M.W.S. by a grant from the U.S. Department of Energy, administered by the Ames Laboratory at Iowa State University. The web site http://diref.uwaterloo.ca/ was used to update the references (ref 86).

Supporting Information Available: Figures 1S−4S giving VH, NbH, TaH, and ScH and YH potential energy curves. This material is available free of charge via the Internet at http://pubs.acs.org.

References and Notes

(1) *J. Comput. Chem.* **2002**, *23*, the 8th issue.

(2) Ermler, W. C.; Ross, R. B.; Christiansen, P. A. *Adv. Quantum Chem.* **1988**, *19*, 139.

(3) Yarkony, D. R. *Int. Rev. Phys. Chem.* **1992**, *11*, 195.

(4) Hess, B. A.; Marian, C. M.; Peyerimhoff, S. D. In *Modern Electronic Structure Theory*; Yarkony, D. R., Ed.; World Scientific: Singapore, 1995; Part I , p 152.

(5) Marian C. M. *Problem Solving in Computational Molecular Science*; Wilson, S., Deircksen G. H. F., Eds.; Dordrecht, Kluwer Academic: Dordrecht, The Netherlands, 1997; p 291.

(6) Marian, C. M. *Reviews in Computational Chemistry*; Lipowitz, K. B., Boyd, D. B., Eds.; Wiley-VCH: New York, 2001; Vol. 17, p 99.

(7) Fedorov, D. G.; Koseki, S.; Schmidt, M. W.; Gordon, M. S. *Int. Rev. Phys. Chem.* **2003**, *22*, 551.

(8) Powell, D.; Brittain, R.; Vala, M. *Chem. Phys.* **1981**, *58*, 355.

(9) (a) Bauschlicher, C. W.; Bagus, P. S.; Nelin, C. J. *Chem. Phys. Lett.* **1983**, *101*, 229. (b) Langhoff, S. R.; Bauschlicher, C. W., Jr. *J. Chem. Phys.* **1988**, *89*, 2160. (c) Langhoff, S. R.; Bauschlicher, C. W., Jr. *Astrophys. J.* **1990**, *349*, 369.

(10) Bauschlicher, C. W.; Langhoff, S. R. *Acc. Chem. Res.* **1989**, *22*, 103.

(11) Dyke, J. M.; Gravenor, B. W.; Josland, G. D.; Lowis, R. A.; Morris, A. *Mol. Phys.* **1984**, *53*, 465.

(12) Doetz, K. H.; Fischer, H.; Hoffman, P.; Kreissl, F. R.; Schubert, U.; Weiss, K. *Transition metal carbene complexes*; Verlag Chemie: Deerfield Beach, FL, 1984.

(13) Simard, B.; Mitchell, S. A.; Humphries, M. R.; Hackett, P. A. *J. Mol. Spectrosc.* **1988**, *129*, 186.

(14) Armentrout, P. B.; Sunderlin, L. S. *Acc. Chem. Res.* **1989**, *22*, 315.

(15) Merer, A. J. *Annu. Rev. Phys. Chem.* **1989**, *40*, 407.

(16) Steimle, T. C.; Shirley, J. E.; Jung, K. Y.; Russon, L. R.; Scurlock, C. T. *J. Mol. Spectrosc.* **1990**, *92*, 4724.

(17) Balasubramanian, K. *J. Chem. Phys.* **1990**, *93*, 8061 and references therein.

(18) Gustavson, T.; Amiot, C.; Verges, J. *J. Mol. Spectrosc.* **1991**, *145*, 56.

(19) Parshall, G. W.; Ittel, S. D. *Homogeneous Catalysis*; Wiley Inerscience: New York, 1992.

(20) Fehlner, T. P. *Inorganiometallic Chemistry*; Plenum Press: New York, 1992.

(21) Dyall, K. G. *J. Chem. Phys.* **1993**, *98*, 9678 and references therein.

(22) Koseki, S.; Schmidt, M. W.; Gordon, M. S. *J. Phys. Chem.* **1992**, *96*, 10768.

(23) Koseki, S.; Gordon, M. S.; Schmidt, M. W.; Matsunaga. N. *J. Phys. Chem.* **1995**, *99*, 12764.

(24) Matsunaga, N.; Koseki, S.; Gordon. M. S. *J. Chem. Phys.* **1996**, *104*, 7988.

(25) Koseki, S. Unpublished results for the sixth-row typical elements: Z_{eff}(Cs) = 12210, Z_{eff}(Ba) = 12432, Z_{eff}(Tl) = 9153, Z_{eff}(Pb) = 18204, Z_{eff}(Bi) = 18426, Z_{eff}(Po) = 18648, Z_{eff}(At) = 18870.

(26) Koseki, S.; Schmidt, M. W.; Gordon, M. S. *J. Phys. Chem.* **1998**, *102*, 10430.

(27) Koseki, S.; Fedorov, D. G.; Schmidt, M. W.; Gordon, M. S. *J. Phys. Chem. A* **2001**, *105*, 8262.

(28) Koseki, S.; Ishihara, Y.; Umeda, H.; Fedorov, D. G.; Gordon, M. S. *J. Phys. Chem. A* **2002**, *106*, 785.

(29) Schmidt, M. W.; Baldridge, K. K.; Boatz, J. A.; Elbert, S. T.; Gordon, M. S.; Jensen, J. H.; Koseki, S.; Matsunaga, N.; Nguyen, K. A.; Su, S.; Windus, T. L.; Dupuis, M.; Montgomery, J. A., Jr. *J. Comput. Chem.* **1993**, *14*, 1347.

(30) Fletcher, G. D.; Schmidt, M. W.; Gordon, M. S. *Adv. Chem. Phys.* **1999**, *110*, 267.

(31) Ruedenberg, K.; Schmidt, M. W.; Dombek, M. M.; Elbert, S. T. *Chem. Phys.* **1982**, *71*, 41, 51, 65.

(32) Schmidt, M. W.; Gordon, M. S. *Annu. Rev. Phys. Chem.* **1998**, *49*, 233.

(33) Lengfield, B. A., III; Jafri, J. A.; Phillips, D. H.; Bauschlicher, C. W., Jr. *J. Chem. Phys.* **1981**, *74*, 6849.

(34) ^{4}F (Group 5) and ^{2}D (Group 3) have $(nd)^3[(n+1)s]^2$ and $(nd)^1[(n+1)s]^2$, respectively.

(35) The SOCI calculations in the ECP approaches for Group 5 hydrides include 684 225 configuration state functions and their spin−orbit matrices include 128 (VH), 240 (NbH), and 275 (TaH) adiabatic states. When the dsds active space is used, the number of configuration state function is 1 470 976 and the dimension of spin−orbit coupling matrices is 234. These numbers for Group 3 hydrides are 209 575 (configuration state functions), 168 (ScH), 204 (YH), and 250 (LaH).

(36) Stevens, W. J.; Krauss, M. *Chem. Phys. Lett.* **1982**, *86*, 320.

(37) Stevens, W. J.; Basch, H.; Krauss, M. *J. Chem. Phys.* **1984**, *81*, 6026.

(38) Stevens, W. J.; Basch, H.; Krauss, M.; Jasien, P. *Can. J. Chem.* **1992**, *70*, 612.

(39) Cundari, T. R.; Stevens, W. J. *J. Chem. Phys.* **1993**, *98*, 5555.

(40) Ehlers, A. W.; Boehme, M.; Dapprich, S.; Gobbi, A.; Hoellwarth, A.; Jonas, V.; Koehler, K. F.; Stegmann, R.; Veldkamp, A.; Frenking, G. *Chem. Phys. Lett.* **1993**, *208*, 111. (a) Exponents of 1.335, 0.835, and 0.591 are used for f functions on Sc, Y, and La, respectively. (b) Exponents of 1.751, 0.952, and 0.790 are used for f functions on V, Nb, and Ta, respectively.

(41) The p exponent is 1.0 for hydrogen.

(42) The effective nuclear charges of Sc, Y, and La atoms are set to 8.61, 184.86, and 803.7, respectively. Those of V, Nb, and Ta atoms are 10.58, 199.26, and 1049.74, respectively. See ref 26.

(43) Huzinaga, S.; Andzelm, J.; Klobukowski, M.; Radzio-Andzelm, E.; Sakai, Y.; Tatewaki, H. *Gaussian Basis Sets for Molecular Calculations*; Elsevier: Amsterdam, The Netherlands, 1984. The present study employs the basis sets consisting of three Gauss-type functions.

(44) Three p exponents are set as (0.236, 0.059, 0.01475) on Sc, (0.212, 0.053, 0.01325) on Y, and (4.0, 1.0, 0.25) on H. Those are set as (0.284, 0.071, 0.01775) on V and (0.26, 0.065, 0.01625) on Nb and Ta, respectively. See refs 29 and 43.

(45) Nakajima, T.; Hirao, K. *Chem. Phys. Lett.* **1999**, *302*, 383.

(46) Fedorov, D. G.; Nakajima, T.; Hirao, K. *Chem. Phys. Lett.* **2001**, *335*, 183.

(47) Colbert, D. T.; Miller, W. H. *J. Chem. Phys.* **1992**, *96*, 8061.

(48) $V(^4F_{9/2})$ correlates to $\Omega = 5$ originating mainly from the excited adiabatic state $^5\Phi$.

(49) Barone, V.; Adamo, C. *Int. J. Quantum Chem.* **1997**, *61*, 443.

(50) Das, G. *J. Chem. Phys.* **1981**, *74*, 5766.

(51) Walch, S. P.; Bauschlicher, C. W. *J. Chem. Phys.* **1983**, *78*, 4597.

(52) Ohanessaian, G.; Goddard, W. A., III *Acc. Chem. Res.* **1990**, *23*, 386.

(53) Bauschlicher, C. W.; Langhoff, S. R. *Transition Metal Hydrides*: *Structure and Bonding*; Dedieu, A., Ed.; VCH Publishers Inc.: New York, 1992; p 103.

(54) Sallans, L.; Lane, K.; Squires, R. R.; Freiser, B. S. *J. Am. Chem. Soc.* **1985**, *107*, 4379.

(55) Aristov, N. Ph.D. Thesis, University of California, Berkeley, 1986.

(56) Moore, C. E. Atomic Energy Levels. In *National Standard Reference Data Series*; National Bureau of Standards: Washington, DC, 1949, 1952, 1958; Vols. I−III, No. 35.

(57) When the larger active space is used in VH and TaH, orbital flip between the active and external spaces occurs in VH and TaH as the internuclear distance becomes shorter. Accordingly, such an active space could not be employed for VH and TaH.

(58) Balasubramanian, K. *J. Chem. Phys.* **1990**, *93*, 8061.

(59) Langhoff, S. R.; Pettersson, L. G. M.; Bauschlicher, C. W., Jr.; Partridge, H. *J. Chem. Phys.* **1987**, *86*, 268.

(60) Das, K. K.; Balasubramanian, K. *J. Mol. Spectrosc.* **1990**, *144*, 245.

(61) Siegbahn, P. E. M. *Theor. Chim. Acta* **1993**, *86*, 219.

(62) Cheng, W.; Balasubramanian, K. *J. Mol. Spectrosc.* **1991**, *149*, 99.

(63) Wittborn, C.; Wahlgren, U. *Chem. Phys.* **1995**, *201*, 357.

(64) Anglada, J.; Bruna, P. J.; Peyerimhoff, S. D. *Mol. Phys.* **1989**, *66*, 541.

(65) (a) Ram, R. S.; Bernath, P. F. *J. Chem. Phys.* **1996**, *105*, 2668. (b) Ram, R. S.; Bernath, P. F. *J. Mol. Spectrosc.* **1997**, *183*, 263.

(66) Balasubramanian, K.; Wang, J. Z. *J. Mol. Spectrosc.* **1989**, *133*, 82.
(67) Guo, J.; Goodings, J. M. *J. Mol. Struct.* **2001**, *549*, 261.
(68) Ram, S.; Bernath, P. F. *J. Chem. Phys.* **1994**, *101*, 9283.
(69) Ram, R. S.; Bernath, P. F. *J. Chem. Phys.* **1996**, *104*, 6444.
(70) Laerdahl, J. K.; Faegri, K., Jr.; Visscher, L.; Saue, T. *J. Chem. Phys.* **1998**, *109*, 10806.
(71) Pyykkö, P. *Chem. Rev.* **1988**, *88*, 563.
(72) Jakubek, Z. J.; Nakhate, S. G.; Simard, B.; Balfour, W. J. *J. Mol. Spectrosc.* **2002**, *211*, 135.
(73) Jakubek, Z. J.; Simard, B.; Balfour, W. J. *Chem. Phys. Lett.* **2002**, *351*, 365.
(74) Bernard, A.; Chevillard, J. *J. Mol. Spectrosc.* **2001**, *208*, 150.
(75) Chen, Y.-M.; Clemmer, D. E.; Armentrout, P. B. *J. Chem. Phys.* **1993**, *98*, 4929.
(76) Casarrubios, M.; Seijo, L. *J. Chem. Phys.* **1999**, *110*, 784.
(77) Chong, D. P.; Langhoff, S. R.; Bauschlicher, C. W., Jr.; Walch, S. P.; Partridge, H. *J. Chem. Phys.* **1986**, *85*, 2850.
(78) Kant, A.; Moon, K. A. *High Temp. Sci.* **1981**, *14*, 23.
(79) Wang, X.; Chertihin, G. V.; Andrews, L. *J. Phys. Chem. A* **2002**, *106*, 9213.
(80) Jeung, G. H.; Koutecky, J. *J. Chem. Phys.* **1988**, *88*, 3747.
(81) Das, K. D.; Balasubramanian, K. *Chem. Phys. Lett.* **1990**, *172*, 372.
(82) Wang, S. G.; Schwarz, W. H. E. *J. Phys. Chem.* **1995**, *99*, 11687.
(83) Kuechle, W.; Dolg, M.; Stoll, H. *J. Phys. Chem. A* **1997**, *101*, 7128.
(84) Hong, G.; Dolg, M.; Li, L. *Chem. Phys. Lett.* **2001**, *334*, 396.
(85) Cao, X.; Dolg, M. *J. Mol. Struct.* **2002**, *581*, 139.
(86) Bernath, P. F.; McLeod, S. *J. Mol. Spectrosc.* **2001**, *207*, 287.